Design of a high capacity Electro Permanent Magnetic adhesion for climbing robots

Conference Paper · December 2012

DOI: 10.1109/ROBIO.2012.6490969

2 authors, including:

Peter Ward
University of Technology Sydney
6 PUBLICATIONS **63** CITATIONS

SEE PROFILE

Proceedings of the 2012 IEEE
International Conference on Robotics and Biomimetics
December 11-14, 2012, Guangzhou, China

Design of a High Capacity Electro Permanent Magnetic Adhesion for Climbing Robots

Peter Ward, Dikai Liu

***Abstract*— The interest for robotic solutions to perform inspection and maintenance of steel structures is realised with reduced costs, improved safety and improved efficiency. However current robotic solutions are limited by the required adhesion to support the robot and payload device. The design of an Electro Permanent Magnetic device is studied to yield a high capacity adhesion method for use with industrial climbing robots. The adhesion device must provide a lightweight, low power and a failsafe solution for ferromagnetic surfaces. The design process to achieve maximum holding force for Electro Permanent Magnets is presented.**

I. INTRODUCTION

The inspection and maintenance of steel structures is a essential to achieve their intended service life. "The periodical inspection, maintenance and cleaning of these infrastructures involve a high number of dangerous manual operations and represent a danger even for skilled workers" [1]. Furthermore inspection and maintenance is time consuming and costly.

For these reasons robotic solutions have been recognised for their potential in the field of inspection and maintenance. Safety concerns for human inspectors are alleviated, efficiency and accuracy of inspection can be improved, costs can be reduced, and new techniques can be introduced. While the potential for inspection robots across many industries has been realised, there are many challenges which must be overcome before they can be delivered successfully. Consideration for the environmental and operational constraints is critical when determining the type of robot, in particular the size, method of locomotion and type of adhesion.

For the inspection of complex steel structures there are several important environmental considerations which have been identified and can be observed in Fig. 1.

- Structures are ferromagnetic
- Surface conditions are rough with build-up of paint, dirt, rust and pitting
- Presence of densely riveted sections
- Unknown regions requiring navigation through and around obstacles

With the environmental constraints in mind, the following operational goals for an adhesion mechanism are considered critical.

- Lower power requirement to increase operational time and remove need for tethered power supply

This work is supported by the Australian Research Council and Roads and Maritime Services NSW

P.K. Ward and D.K. Liu are with the Centre for Autonomous Systems, University of Technology, Sydney, NSW 2007, Australia
Peter.K.Ward@student.uts.edu.au,
Dikai.Liu@uts.edu.au

(a) (b)

Fig. 1: *a)* Complex bridge lattice *b)* Heavy rusting and paint peel [2]

- Failsafe to prevent robot detaching in event of power failure
- Light weight to reduce overall system weight and adhesion requirements
- Support light climbing robot and payload such as camera and sensors
- Compliant on rough surfaces

A. Adhesion Methods

The method of adhesion is one of the most challenging design aspects for climbing robots. Given the environmental and operational constraints mentioned previously, there are a wide variety of adhesion methods to consider including biologically inspired, electrostatic, mechanical, suction and magnetic.

1) Biologically Inspired: Biologically inspired adhesion such as synthetic gecko skin is light weight, low power and power failsafe. This adhesion provides high shear force, however being unidirectional in nature means the robot will have difficulties traversing a plane in any arbitrary direction. A recent research has shown that the deterioration of the gecko skin to be of concern, with a significant reduction in shear force strength observed with high cycles [3]. This is a concern due to the intended operational time spent on the bridge and required number of steps to traverse it. Another study has also shown that further "research into self-cleaning or contamination resistance is required" [4] for effective long term use, which is of concern for the harsh environments intended.

2) Electrostatic: Electrostatic adhesion delivers the advantages of surface independence, light weight and low power, however, it typically requires extremely flat contact surfaces for adhesion. Recent methods using a flexible electroadhesive clamping method [5] is capable of achieving

978-1-4673-2126-6/12/$31.00 © 2012 IEEE

high adhesion strength and compliance to rough surfaces. The technology was demonstrated using an inch-worm robot on steeply inclined surfaces. However, it has been noted it is susceptible to peeling and hence best suited to tank style locomotion to minimise loading in peel direction. Due to the complex structures and inverted sections expected, an adhesion device less susceptible to peeling is required.

3) Mechanical: Mechanical adhesion can provide high holding capacity and failsafe techniques for adhesion. However, it typically requires more power and is much heavier than other forms of adhesion. Furthermore the adhesion is limited to structures where there are graspable features such as girders and pipes, as demonstrated with [6]. These methods are task specific and can not accommodate flat regions. Another example shows modifications to the environment where an inchworm robot uses docking stations for adhesion and power [7]. However this is not an ideal solution for inspection in unknown areas and would require consideration at the design stage for the steel structures.

4) Suction/Vacuum: Various methods of suction and vacuum techniques exist, however they are limited in their ability with plane transitions. Open suction methods are capable of traversing rough surfaces [8]. However, they are not capable of performing plane transitions, provide less stability and are not power failsafe. In order to perform plane transfers, inchworm robots with sealed active suctions cups are typically used for increased stability. Active suction methods typically use an external air compressor with tethered air lines in order to minimise the robot's weight. Sealed suction cups also require smooth surfaces as surface discrepancies and roughness reduce effectiveness. An inchworm robot has been demonstrated [9] using suction cups however its performance on rough surfaces is limited and fail safety is not ensured.

5) Magnetic: Steel structures have "a limit to the thickness of paint that can be applied to a surface before it starts to fall off" [10] as can be observed in Fig. 1(b). This is a serious concern when considering forms of adhesion which rely on direct adhesion to the top surface layer. Direct adhesion to the paint may cause it to peel off and consequently fail in adhesion. Magnetic adhesion on the other hand can provide a high capacity and failsafe adhesion in which the holding force is maintained within the ferromagnetic structure itself, rather than the top surface layer. Magnetic adhesion is however limited by the effective air gap due to the build-up of paint, rust and dirt.

While electromagnets require a continuous power supply and hence, does not provide power failsafe operation, permanent magnetic solutions show the greatest feasibility. In using permanent magnets the greatest problem is removing the magnet from the surface to allow motion to occur. Two permanent magnetic devices which solve this issue have been identified, investigated and appear feasible for the intended application, satisfying the design requirements.

The Magnetic Switchable Device (MSD) [11] is able to switch between ON and OFF states by the means of rotating a magnet using an actuator as shown in Fig. 2. A 22.4 g unit has been shown to achieve a holding force of 150 N using only 18.9 mJ.

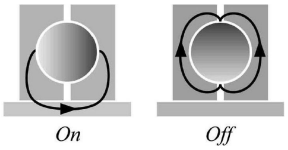

Fig. 2: Classic parallel configuration for Magnetic Switchable Device [11]

Another approach for switching between ON and OFF states is realised in the Electro Permanent Magnet (EPM) [12]. The solid-state device is switched using a short high current pulse to remagnetise one of the magnetic cores contained within the device, as observed in Fig. 3. The EPM has been demonstrated as a latch for millimetre scale modular robotic systems. This assembly has a maximum holding force of 4.4 N at a weight of 0.2 g and switching speed of 300μsec using only 5 mJ [12]. Significant weight is saved in comparison to electromagnets which require thicker, high density wire to withstand the continuous applied current. Furthermore, the magnetic state is preserved with no further power required, hence power fail safe.

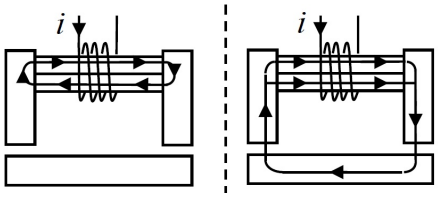

Fig. 3: OFF and ON states for the EPM [12]

While both of these adhesion methods appear suitable, the EPM is attractive due to its fast switching speed and solid state, requiring no mechanical actuators. The research presented in this paper shows the EPM scaled for use in climbing robots on ferromagnetic surfaces, a method for achieving the maximum holding force, the test results and conclusions.

II. DESIGN AND FORMULATION

A. Electro Permanent Magnet Design

To maximise the magnetic holding force of the EPM, design parameters including magnet grade, shape, size, and magnetic fixture properties have been taken into consideration.

An EPM requires two magnetic cores. The ability to control the magnet lies in the coercivities of the magnets; where coercivity is the magnetising field required to bring the maximum residual magnetic strength to zero i.e. demagnetise it. One magnetic core is a hard Neodymium-Iron-Born (NdFeB), the other is a semi-hard Aluminum-Nickel-Cobalt (AlNiCo) core. While these magnets share the same residual magnetic flux densities (B_r = 1.35 T) they greatly vary in coercivities (H_{ci}). The 60 kA/m coercivity for the chosen AlNiCo core requires significantly less field intensity

to demagnetise in comparison to the 1114 kA/m required for the chosen NdFeB . Hence, AlNiCo is referred to as the switching magnet.

Fig. 4 considers a plane between the target surface and the magnetic fixtures. The magnetic fixtures, referred to as keepers, are of ferromagnetic matierial in order to redirect the magnetic flux. By considering the flux in the normal direction z for a single keeper, we can use the Maxwell Stress Tensor to represent the magnetostatic stress,

$$S_z = \frac{B_z^2}{2\mu_0}$$

where S_z is the magnetostatic stress, μ_0 is the permeability of free space ($\mu = 4\pi 10^{-7}$), and B_z is the flux density normal to the surface.

If we consider the pole area, A, of a single keeper in contact with the target surface, then the force, being stress per unit area becomes,

$$F_z = \frac{B_z^2 A}{2\mu_0}.$$

As the EPM device has two keepers, we consider the flux density and area for each keeper and hence the force F required to move the assembly away from a ferromagnetic surface becomes,

$$F = \frac{1}{2\mu_0}(B_1^2 A_1 + B_2^2 A_2).$$

If both keepers have equal magnetic flux density B and pole area A,

$$F = \frac{B^2 A}{\mu_0}. \tag{1}$$

It can be noted that the force is strongly related to the magnetic flux density through the squared factor, hence for a particular sized magnet it is important to maximise this magnetic flux density of the keepers.

By Gausss law for Magnetism, the total flux entering a volume will equal the total flux leaving the volume. Therefore, if we consider the volume of a keeper, flux which enters the keeper from the magnets is directed through the keeper to the surface. The flux conservation can be expressed as,

$$B_{InKeeper} A_{InKeeper} = B_{OutKeeper} A_{OutKeeper}$$

$$2A_{Magnet} B_{Magnet} + \Phi_{Leakage} = A_{Keeper} B_{Keeper} + \Phi_{Leakage} \tag{2}$$

where both magnets have equal pole area and magnetic flux density.

Ferromagnetic materials have a property known as the magnetic saturation, where any further increases in the applied magnetic field will not yield any significant increase in the flux density of that material. By designing to achieve this magnetic saturation $B_{Saturation}$ in the keeper, a keeper area A_{Keeper} which maximises the holding force can be determined. It can be assumed the flux leakage $\Phi_{Leakage}$ is minimal for cases where the air gap approaches zero.

$$B_{Keeper} = B_{Saturation}$$

$$\Phi_{Leakage} = 0$$

From (2),

$$A_{Keeper} = \frac{2A_{Magnet} B_{Magnet}}{B_{Saturation}} \tag{3}$$

By combining (1) and (3) the maximum holding force required to move the EPM away from the surface can then be calculated,

$$F_{Maximum} = \frac{B_{Saturation}^2 A_{Keeper}}{\mu_0}. \tag{4}$$

The maximum holding force is now limited by the magnetic flux saturation point for the keepers and the keeper area. The keeper area (3) is related to the diameter of the magnets and the length of the keeper, see Fig. 6. Using a 10 mm diameter for both magnets an EPM design curve, seen in Fig. 5, has been developed using (4). The curve highlights the effect on the maximum holding force with changes in keeper length, for various keeper materials. Three keeper materials with magnetic saturations points of 1 T, 1.3 T and 2.2 T are compared.

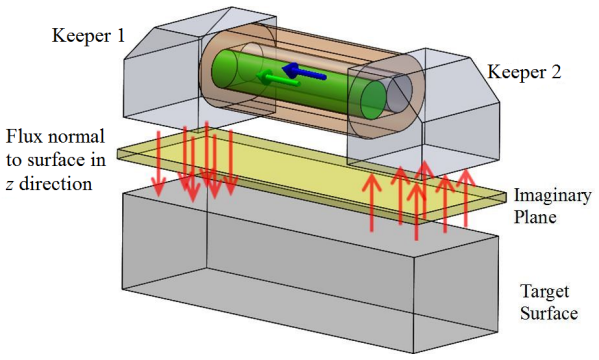

Fig. 4: Flux crossing plane between keepers and surface in normal direction for small air gaps

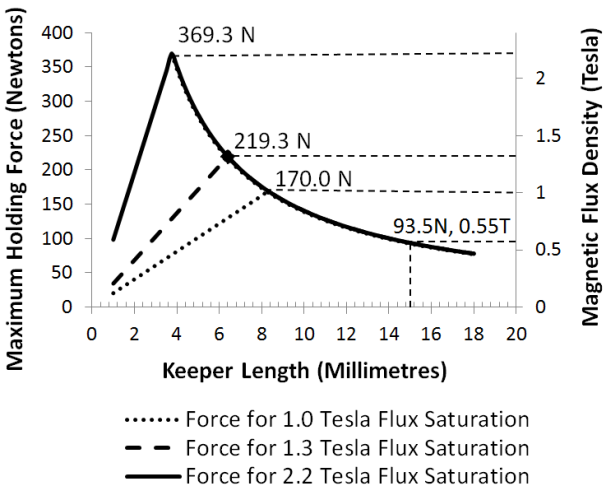

Fig. 5: EPM design curve shows effect on holding force with changes in keeper length for three different keeper materials.

It can be observed that with an insufficient keeper length magnetic saturation occurs in the keeper and the force is limited. At the ideal keeper length, the holding force is at a maximum. Further increases in the keeper length lead to a decay in the flux density and hence, the maximum holding force.

B. Construction

The constructed EPM is pictured in Fig. 6. Both cores have a diameter of 10mm and residual magnetic flux density of 1.35 T. Ideally keepers were to be constructed from a material with a magnetic saturation of 2.2 T however readily available construction steel with a magnetic flux saturation of approximately 1.3 T was used for the initial prototype. A keeper width w of 25 mm and keeper height h of 14 mm was used to contain the two cores side by side with room for coil windings. A less than ideal keeper length l of 15 mm was used with a countersunk depth c of 5 mm for structural support. The EPM device weighs 96 grams. Based on the EPM design curve in Fig. 5 a keeper length of 6.4 mm should have been used in order to achieve the maximum force for the given magnets and keeper material. The design curve shows an expected holding force of 93.5 N for the 15 mm keepers used.

C. Simulation

Magnetostatic Finite Element Analysis (MFEA) has been used to model the magnetic flux density with different keeper lengths. A comparison between the ideal design using 6.4 mm keeper lengths, shown in Fig. 7(a), and the constructed EPM with 15 mm keeper lengths, shown in Fig. 7(b). A significant difference in flux saturation is observed internally through the keepers and the target surface. Simulated surface plots showing the magnetic flux density for the ideal and constructed keepers can be seen in Fig. 7(c). For the optimised keepers the poles reach saturation with average of 1.18 T per pole with a corresponding theoretical maximum holding force of 221.6 N. The constructed keepers do not reach saturation, yielding 0.55 T per pole with a corresponding theoretical maximum holding force of 90.27 N. These results correlate closely to the theoretical EPM design curve, Fig. 5.

D. Control Circuit

To fully remagnetise the AlNiCo core a saturating magnetic field intensity (H_sat) of three to five times the intrinsic coercivity is required. For the AlNiCo LNG60, this correlates to (H_sat) = 180 kA/m. Based on the length of the magnet, a magnetising pulse of 51.4 A is required using 116 turns of 24 AWG insulated copper wire. The current is delivered from a 10 000 F capacitor charged to 32.25 V. An estimated pulse width of 4.5 ms is required to ensure the magnet is completely saturated. An Atmel AVR is used to control two BTN7970 half bridge drivers. Fig. 8 shows the equipment and test setup used to test the EPM.

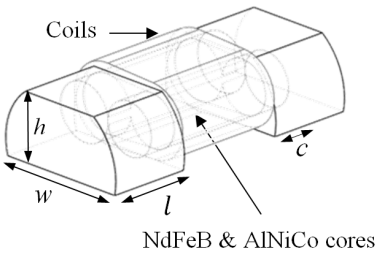

Fig. 6: Electro Permanent Magnet design

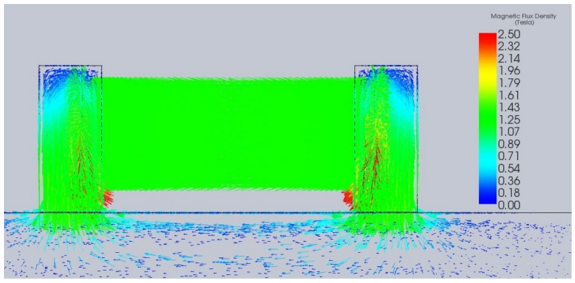

(a)

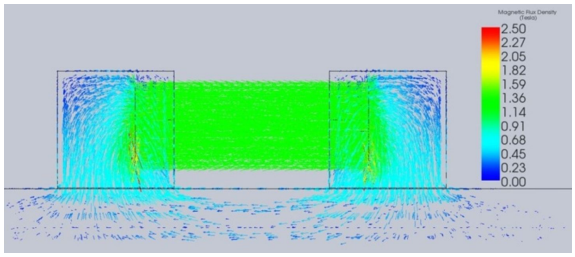

(b)

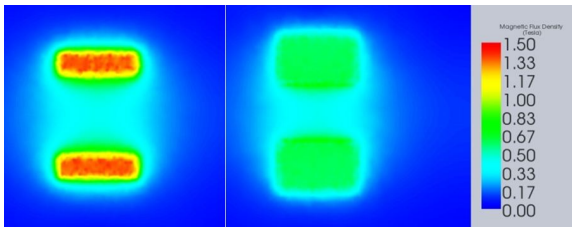

(c)

Fig. 7: *a)* MFEA highlights magnetic flux through ideal EPM assembly with keepers 6.4 mm in length. *b)* MFEA highlights magnetic flux through constructed EPM assembly with keepers 15 mm in length. *c)* MFEA compares surface flux of ideal keepers and constructed keepers.

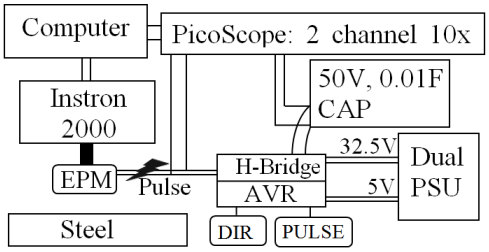

Fig. 8: Test setup

III. EXPERIMENTS AND RESULTS

A. Holding Force

To determine the maximum holding force an initial pulse voltage of 15 V was used, with increments of 2-3 V for successive tests. After each pulse a pull test was conducted and the peak holding forces were recorded, Fig. 9.

The desired voltage of 32.25 V was not achieved. Although within theoretical safe limits the magnetising circuit would not deliver pulses beyond 27 V, 43 A. A maximum force of 82.2 N was recorded at this level, however it is expected that the force would reach theoretical limit using a higher pulse voltage. The maximum pulse voltage was limited to 25 V for subsequent tests.

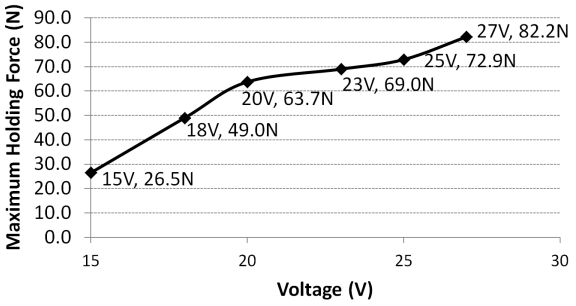

Fig. 9: Effect on maximum holding force with increased pulse voltage, using a pulse length of 4 ms

B. Pulse Duration

Pulse lengths were varied between 0.5 ms to 4 ms to study the effects on holding force. Pulses lengths greater than 2.4 ms led to a magnetising fields too low to have effect on the AlNiCo and hence showed no noticeable increase in holding force. The required energy for a 2.4 ms pulse length is 1.89 J.

C. OFF State

Switching the magnet off effectively reduces the holding force of the EPM by containing all the magnetic flux internally. A maximum of 4.7 N was recorded in the off state. It is expected with a larger pulse voltage this would approach zero as the AlNiCo core reaches the same residual flux density at the NdFeB core.

D. Repeatability

In order to determine the repeatability of the results, 5 tests were conducted using the same pulse characteristics. The EPM was switched off with a reverse pulse between tests. The average holding force achieved was 74.7 N with a standard deviation of 0.5 N.

E. Stability

The performance of the EPM was tested by allowing it to rest in contact with a steel surface for extended periods of time. After 25 minutes a holding force of 73.7 N was recorded, a waiting period of 2 hours yielded 74.2 N demonstrating no loss in holding force. The EPM successfully supported a 5kg weight for a two week period before the test was stopped. When the EPM was left suspended in air for 5 hours the effect of self-demagnetisation is apparent with a final holding force settling to 42 N. This is due to the strength of the NdFeB partially demagnetising the AlNiCo core. This is inconsequential as the device can simply be pulsed again when the full adhesion force is required.

F. Air Gaps

To simulate the expected air gaps from dirt, rust and paint, the maximum holding force has been recorded at increasing distance from the surface. Fig. 10 shows the reduced holding force as the air gap increases. An effective holding force of approximately 35% maximum holding force is experienced at 1 mm.

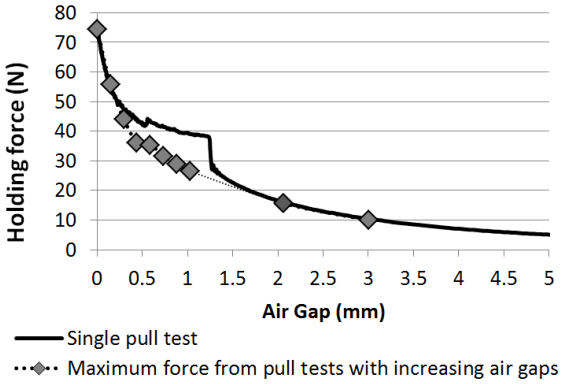

Fig. 10: Effect on holding force with increased air gaps

IV. DISCUSSION AND FUTURE WORKS

A. Discussion of Results

The experimental results show a maximum holding force of 82.2 N being 87.9% of the theoretical holding force of 93.5 N. This has been achieved using a pulse voltage of 27 V, being 83% of the theoretical 32.5 V required to completely magnetise the core. It is expected that a new magnetising circuit capable of reliably delivering the required pulse voltage will achieve experimental results closer to that specified in the EPM design curve.

The larger keeper length has also contributed to a holding force less than the theoretical maximum. Further testing with a keeper length specified by the EPM design curve is expected to improve results. The reduction in holding force with a 1 mm air gap is a concern for the intended application, hence more accurate factors of safety can be implemented and improved designs can be considered.

B. Integration of Electro Permanent Magnets

With the ability to control the magnetic state of the EPM at high speeds, there are many climbing robot designs which have been envisioned. Furthermore, these designs provide power-fail safe adhesion, ability to clean ferromagnetic material from the adhesion, safe attachment, detachment and transport of the climbing robot.

One envisioned method of integration for the EPMs is in a rigid housing, to be better suited for legged robots where greater stability is required Fig. 11(a). The fast switching

speeds allow for fast walking gaits without increased joint torques to remove the feet, as experienced by [13]. In the case of a bipedal or inchworm robot, the OFF state of the EPM devices provide a safe configuration space close to the end effector allowing greater maneuverability for inspection in tight spaces Fig. 11(b). Furthermore the device can be switched completely off with no residual force, which has been an issue when using electromagnets [14].

The EPM also improves the implementation for magnetic adhesion in flexible membranes such as polyurethane. The flexibility provides greater surface compliance as has been achieved with tank type climbing robots. The ability to individually control the EPMs may reduce the peeling moments through deactivating the adhesion before the EPM leaves the surface Fig. 11(c). This overcomes the problem in adhesive tracks where belt tightness must be optimised or a tail is required to prevent this peeling moment while driving, as noted by [15], [16] and [17].

Furthermore a flexible membrane can also be used in caterpillar type robots where sliding or shuffle steps are used. Different body segments can be activated and deactivated as required Fig. 11(d). Other techniques of permanent magnetic switching typically require bulkier and interconnected mechanical components, and hence reduce the flexibility of the robot.

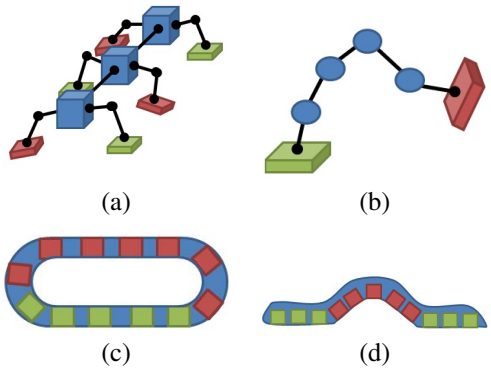

Fig. 11: *a)* Legged concept *b)* Bipedal concept *c)* Tracked concept *d)* Shuffle concept (Green EPM on, Red EPM off)

V. CONCLUSIONS

This research has demonstrated the scalability in the EPM for greater load capacities and has identified areas for improvement. An EPM design curve has been presented which is supported through theoretical analysis, MFEA and experimental results. The EPM is promising for adhesion on ferromagnetic structures where a high capacity, low weight, low power and failsafe solution is required. The use of the EPM is believed to improve previous methods of locomotion and inspire new methods. Several methods of implementing the EPMs have been proposed for future work.

VI. ACKNOWLEDGMENTS

This work is supported by the Australian Research Council (ARC) Linkage Grant (LP100200750), the NSW Roads and Maritime Services, the Centre for Autonomous Systems (CAS) at the University of Technology, Sydney. The authors thank Greg Peters and the rest of climbing robot team for their support and assistance in the project. Cameron Mennie for his assistance constructing the EPMs. Peter Watterson for sharing his wealth of knowledge in magnetic theory. EMWORKS for providing a trial license with EMS.

REFERENCES

[1] A. G. C. Balaguer and A. Jardon, "Climbing robots mobility for inspection and maintenance of 3d complex environments," in *Autonomous Robots*, vol. 18. The Netherlands: Springer Science + Business Media, Inc., 2005, p. 157169.

[2] Q. L. Photography, *http://archive.quintinlake.com/*, 2010.

[3] A. G. Gillies and R. S. Fearing, "Shear adhesion strength of thermoplastic gecko-inspired synthetic adhesive exceeds material limits," *Langmuir*, vol. 27, no. 18, pp. 11 278–11 281, Aug 2011. [Online]. Available: http://dx.doi.org/10.1021/la202085j

[4] B. Aksak, M. Murphy, and M. Sitti, "Gecko inspired micro-fibrillar adhesives for wall climbing robots on micro/nanoscale rough surfaces," in *Robotics and Automation, 2008. IEEE International Conference on*, ser. ICRA 2008, Pasadena, USA, May 2008, pp. 3058 –3063.

[5] H. Prahlad, R. Pelrine, S. Stanford, J. Marlow, and R. Kornbluh, "Electroadhesive robots; wall climbing robots enabled by a novel, robust, and electrically controllable adhesion technology," in *Robotics and Automation. IEEE International Conference on*, ser. ICRA, Pasadena, USA, May 2008, pp. 3028–3033.

[6] A. M. L. d. A. A. Tavakoli, M. Marjovi, "3dclimber: A climbing robot for inspection of 3d human made structures," *IEEE/RSJ International Conference on Intelligent Robots and Systems, 2008. IROS 2008.*, pp. 4130–4135, September 22-26 Sept. 2008, nice, France.

[7] A. Huete, J. Victores, S. Martinez, A. Gimenez, and C. Balaguer, "Personal autonomy rehabilitation in home environments by a portable assistive robot," *Systems, Man, and Cybernetics, Part C: Applications and Reviews, IEEE Transactions on*, vol. 42, no. 4, pp. 561 –570, July 2012.

[8] Z. Jiang, J. Li, X. Gao, N. Fan, and B. Wei, "Study on pneumatic wall climbing robot adhesion principle and suction control," in *Robotics and Biomimetics. IEEE International Conference on*, ser. ROBIO, Bangkok, Thailand, Feb 2008, pp. 1812 –1817.

[9] Q. Hong, R. Liu, H. Yang, and X. Zhai, "Wall climbing robot enabled by a novel and robust vibration suction technology," in *Automation and Logistics. IEEE International Conference on*, ser. ICAL, Shenyang, China, Aug 2009, pp. 331 –336.

[10] N. S. W. Road and T. Authority, "Sydney harbour bridge conservation management plan 2007," *Godden Mackay Logan Ltd*, p. 114, 2007.

[11] F. Rochat, P. Schoeneich, M. Bonani, S. Magnenat, F. Mondada, and T. M. O. M. H. V. G. S. Hannes Bleuler Fujimoto, Hideo, "Design of magnetic switchable device (msd) and applications in climbing robot," in *Climbing and Walking Robots and the Support Technologies for Mobile Machines.The 13th International Conference on*, ser. CLAWAR 2010. Nagoya, Japan: World Scientific, Sep 2010, pp. 375–382.

[12] A. N. Knaian, "Electropermanent magnetic conectors and actuators: Devices and their aplication in programable matter," Ph.D. dissertation, Electrical Engineering and Computer Science, Massachusetts Institute of Technology, June 2010.

[13] G. Peters, "Uts rvc: The design and construction of a prototype climbing robot," University of Technology, Sydney. Faculty of Engineering and Infomation Technology. Thesis, Nov 2009.

[14] K. Kotay and D. Rus, "Navigating 3d steel web structures with an inchworm robot," in *Intelligent Robots and Systems '96, IROS 96, Proceedings of the 1996 IEEE/RSJ International Conference on*, vol. 1, nov 1996, pp. 368 –375 vol.1.

[15] G. Lee, G. Wu, S. H. Kim, J. Kim, and T. Seo, "Combot: Compliant climbing robotic platform with transitioning capability and payload capacity," in *Robotics and Automation (ICRA), 2012 IEEE International Conference on*, may 2012, pp. 2737 –2742.

[16] H. Prahlad, R. Pelrine, S. Stanford, J. Marlow, and R. Kornbluh, "Electroadhesive robots; wall climbing robots enabled by a novel, robust, and electrically controllable adhesion technology," in *Robotics and Automation, 2008. ICRA 2008. IEEE International Conference on*, may 2008, pp. 3028 –3033.

[17] W. Shen, J. Gu, and Y. Shen, "Proposed wall climbing robot with permanent magnetic tracks for inspecting oil tanks," in *Mechatronics and Automation, 2005 IEEE International Conference*, vol. 4, july-1 aug. 2005, pp. 2072 – 2077 Vol. 4.